New Journal of Physics
The open-access journal for physics

Thermodynamic properties and resistivity of the ferromagnetic semiconductor EuC_2

O Heyer[1], P Link[2], D Wandner[2], U Ruschewitz[2] and T Lorenz[1,3]

[1] II. Physikalisches Institut, Universität zu Köln, Zülpicher Straße 77, 50937 Köln, Germany

[2] Institut für Anorganische Chemie, Universität zu Köln, Greinstraße 6, 50939 Köln, Germany

E-mail: tl@ph2.uni-koeln.de

New Journal of Physics **13** (2011) 113041 (12pp)
Received 8 August 2011
Published 29 November 2011
Online at http://www.njp.org/
doi:10.1088/1367-2630/13/11/113041

Abstract. EuC_2 is a ferromagnet with a Curie temperature of $T_C \simeq 15$ K. It is semiconducting with the particularity that the resistivity drops by about five orders of magnitude on cooling through T_C, which is therefore called a metal–insulator transition. In this paper, we study the magnetization, specific heat, thermal expansion and the resistivity around this ferromagnetic transition on high-quality EuC_2 samples. At T_C we observe well-defined anomalies in the specific heat $c_p(T)$ and thermal expansion $\alpha(T)$ data. The magnetic contributions of $c_p(T)$ and $\alpha(T)$ can satisfactorily be described within a mean-field theory, taking into account the magnetization data. In zero magnetic field, the magnetic contributions of the specific heat and thermal expansion fulfil a Grüneisen scaling, which is not preserved in finite fields. From an estimation of the pressure dependence of T_C via Ehrenfest's relation, we expect a considerable increase of T_C under applied pressure due to a strong spin–lattice coupling. Furthermore, the influence of weak off-stoichiometries δ in $EuC_{2\pm\delta}$ was studied. It is found that δ strongly affects the resistivity, but hardly changes the transition temperature. In all these aspects, the behaviour of EuC_2 strongly resembles that of EuO.

[3] Author to whom any correspondence should be addressed.

Contents

1. Introduction

Metal dicarbides are composed of a metal ion (M^{n+}) and an acetylide ion (C_2^{2-}). Depending on the metal, their physical properties may vary over a wide range and thus these systems have been investigated for several decades. The electronic and magnetic properties depend on the valence of the metal ion and these compounds can be insulators, metals or superconductors [1]. Within a simple model that fits for alkaline-earth as well as rare-earth dicarbides [2, 3], trivalent or quadrivalent metals form metallic dicarbides, while divalent metals form insulating compounds. Of particular interest, therefore, are metals that can realize both the divalent and the trivalent state, such as, e.g., Eu and Yb. Experimental studies of these systems are, however, rare, which is most probably related to the fact that both EuC_2 and YbC_2 very rapidly decompose in air. Since 1964, several publications have reported the synthesis of EuC_2, but there is still disagreement about whether it crystallizes in a tetragonal [4, 5] or a monoclinic [6, 7] structure at room temperature and below. The tetragonal modification of EuC_2 and its solid solutions with La and Gd were investigated in [5] and it was found that at least some of the results are not consistent with the simple model mentioned above. For example, the magnetization data of EuC_2 reveal a ferromagnetic transition at $T_C \simeq 20\,K$ with a saturation moment of $\simeq 7 \frac{\mu_B}{fu}$. This suggests that europium is in the divalent state and one would expect insulating behaviour, which could not, however, be confirmed by the corresponding measurements of the electrical resistivity. In a more recent work [7], the ferromagnetic order with a somewhat smaller $T_C \simeq 15\,K$ has been confirmed, but the measured electrical resistivity $\rho(T)$ shows activated characteristics within the paramagnetic phase and varies over several orders of magnitude when the sample is heated from T_C to room temperature, whereas, according to [5], $\rho(T)$ is almost temperature independent in that temperature range. Despite these very different temperature dependences of $\rho(T)$, both works agree at least qualitatively in the observation of a strong suppression of ρ in the ferromagnetic ordered phase. The $\rho(T)$ data of EuC_2 presented in [7] strongly resemble those of the much-investigated EuO, which may be viewed as one of the most suitable model systems for future spintronics devices.

In this paper, we present a detailed study of the thermodynamic properties specific heat, magnetization and linear thermal expansion, as well as electrical resistivity measurements of various EuC_2 samples, which were prepared under slightly varying conditions. The analysis of thermodynamic properties revealed that the magnetic ordering transition can be consistently described by assuming localized Eu^{2+} moments with spin $S = 7/2$ that are coupled ferromagnetically. In particular, these data do not yield any indication that the magnetic ordering transition is related to a sizable change of the average valence state of the Eu ions.

For the electrical transport behaviour, we typically found semiconducting behaviour in the paramagnetic phase and a decrease of $\rho(T)$ in the ferromagnetically ordered phase. The $\rho(T)$ curves measured on different samples, however, vary with respect to the absolute value and/or the activation energy. This sample dependence is very much pronounced when the preparation conditions are changed, but—to a lesser extent—is also present for samples prepared under nominally the same conditions.

2. Experimental details

In order to synthesize EuC_2, a total amount of 0.15 or 0.3 g of Eu and graphite powders was mixed in the molar ratio of 1 : 2.2 in a ball mill placed inside an argon-filled glove box. The small surplus of graphite was used to inhibit the formation of EuO and to account for graphite losses due to a reaction with the container wall. Details of the preparation and characterization of EuC_2 can be found in [7]. In addition, we prepared samples with different Eu/C ratios of $1 : 2.2 + x$ in order to get off-stoichiometric samples. Below, we will discuss samples prepared with $x = 0$, -0.1 and 0.3, which are labelled as EuC_2, $EuC_{2-\delta}$ and $EuC_{2+\delta}$. As no significant changes of the lattice parameters were observed by x-ray powder diffraction on these samples, we conclude that the off-stoichiometries are rather small. In order to check whether this route of preparing off-stoichiometric $EuC_{2\pm\delta}$ samples works at all, we also prepared samples for significantly larger variations of the Eu/C ratio (up to $x = \pm 0.8$) and over this larger range we indeed observed a small systematic increase of the unit cell volume. Changing the Eu/C ratio by $\Delta x = 1$ results in an increase of the unit cell volume of about 0.5%, which is clear evidence for off-stoichiometric $EuC_{2\pm\delta}$. However, for $x < -0.3$ we also observe a few per cent of metallic Eu in the diffraction patterns, and for the range $x > 0$ we expect a certain amount of unreacted carbon, which, however, cannot be detected by a laboratory x-ray diffractometer. Therefore, the following studies were restricted to the samples prepared for $-0.1 \leqslant x \leqslant 0.3$, where it is certain that no traces of metallic Eu are detectable in the diffraction patterns and the influence of possible carbon impurities is expected to be negligible.

As already mentioned, EuC_2 very rapidly decomposes when it is in contact with air. Thus, all sample handling was carried out in a glove box with inert atmosphere (Ar, 99.999%). This box was adapted to incorporate various sample rods with measuring cells for the specific heat, the thermal expansion and the electrical resistivity. After the sample was mounted to the respective platform in argon atmosphere, the surrounding tube was evacuated and, for the actual measurements, was put into a ^{4}He bath cryostat equipped with a 14 T magnet. For the measurements at low temperatures (0.3–60 K) we used a ^{3}He evaporator system (Heliox-VL, Oxford Instruments) with home-built devices for heat-capacity and thermal-expansion measurements. The heat-capacity device uses the adiabatic heat-pulse method. The thermal-expansion device is a dilatometer, which works with a variable plate capacitor controlled by the sample length. The resistivity has been measured in the temperature range 5–300 K in a home-built setup that provides a temperature-variable sample platform in vacuum. We used a standard four-probe technique with current and voltage contacts made by a two-component silver epoxy. The magnetization was studied in a physical property measurement system (PPMS; Quantum Design) using a vibrating sample magnetometer in the temperature range 2–300 K in magnetic fields up to 14 T. To keep the sample in an Ar atmosphere during the magnetization measurements, it was sealed in a quartz capillary (Suprasil) inside the glove box.

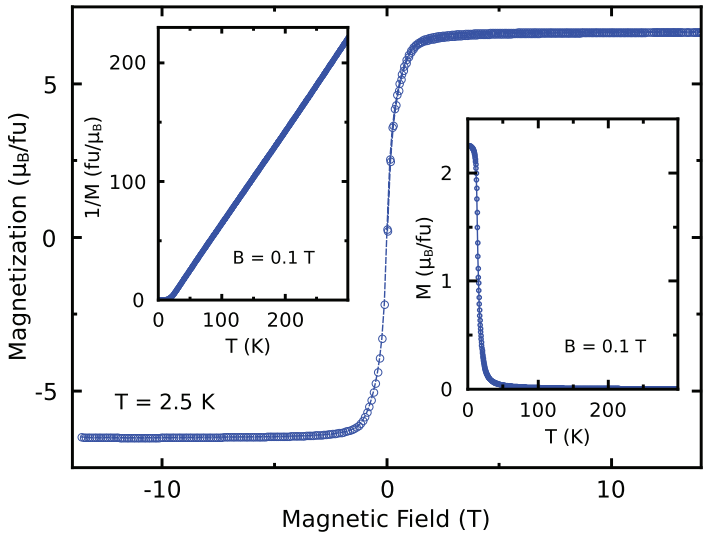

Figure 1. The field-dependent magnetization of EuC_2 shows a soft ferromagnet with a negligible hysteresis and a saturation moment of $\mu_{sat} \simeq 6.7\,\mu_B$. As presented in the insets, the temperature-dependent $M(T)$ follows the Curie–Weiss law in the paramagnetic phase.

3. Results and discussion

Figure 1 displays magnetization data for EuC_2, which was measured over a wide temperature range in an external magnetic field of $B = 0.1$ T and at 2.5 K in the field range of ± 14 T. As illustrated in the left inset of figure 1, the $M(T)$ data are well described by the Curie–Weiss law $M^{-1}(T) = C^{-1}(T - \Theta)$ from 300 K down to about 20 K. Around $T_C \simeq 14$ K, $M(T)$ strongly increases and approaches an almost constant value with further decreasing temperature. The Curie–Weiss fit yields $\Theta = 17.4$ K, i.e. a ferromagnetic exchange coupling, and an effective magnetic moment $\mu_{eff} = 7.56\,\mu_B\,fu^{-1}$. The magnetization curve $M(B)$ at 2.5 K has the typical characteristics of a soft ferromagnet with a very small hysteresis and a saturation moment of $\mu_{sat} \simeq 6.7\,\mu_B\,fu^{-1}$. Both, μ_{sat} and μ_{eff}, agree within about 4% with the values expected for Eu^{2+} with $J = 7/2$ ($\mu_{sat} = 7\,\mu_B$ and $\mu_{eff} = 7.94\,\mu_B$). An important observation is that the sample studied does not show any indication of magnetic impurities. In particular, we can exclude a partial oxidation of the sample, because this would result in contamination with EuO, which would easily be detected in the $M(T)$ measurement because it undergoes a ferromagnetic transition at 69 K.

Figure 2 displays the specific heat measurements in zero field and 14 T. The zero-field data show a pronounced anomaly at $\simeq$14 K, which can be attributed to the ferromagnetic ordering transition and around 4 K a broad maximum is seen in c_p^{0T}/T that resembles a Schottky anomaly[4]. Both features are drastically broadened in the 14 T curve, as expected for a ferromagnet in a large magnetic field. For a quantitative analysis, one has to separate the phononic and magnetic contributions to the total specific heat, $c_{tot} = c_{ph} + c_{mag}$. Because we are interested in c_{mag} we need an estimate of c_{ph} that covers the entire temperature range up to

[4] In [8], a similar Schottky-like anomaly was observed in $GdCu_2$, which shows a non-colinear magnetic structure.

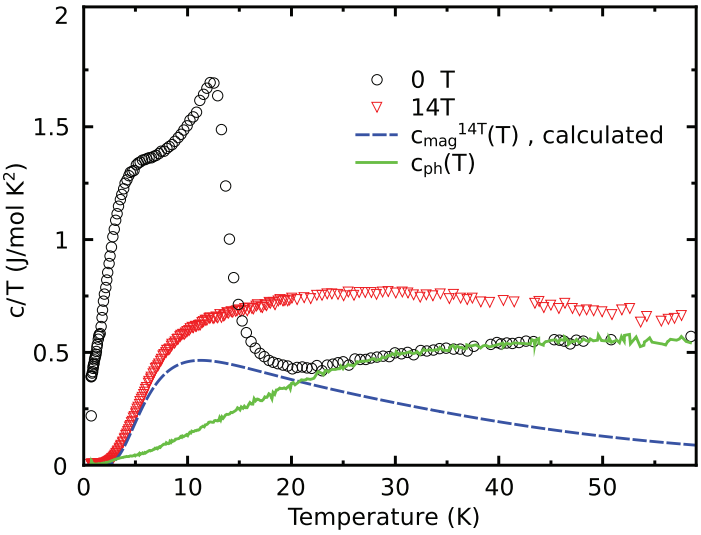

Figure 2. Specific heat measured in zero field and in an external magnetic field of 14 T. The dashed line is the calculated magnetic heat capacity of a ferromagnet in 14 T. The difference between the measured data and the calculated values in 14 T shown as a solid line represents the phonon contribution (see text).

60 K. For this estimate we calculate the magnon contribution $c_{\mathrm{mag}}^{14\,\mathrm{T}}(T)$ for our largest magnetic field of 14 T within a mean-field approximation and subtract it from the experimental data. As the phonon contribution can be expected to be independent of the magnetic field, this difference represents c_{ph} for all applied fields. The calculated $c_{\mathrm{mag}}^{14\,\mathrm{T}}/T$ is shown by the dashed line in figure 2 and the solid line displays the obtained c_{ph}/T, which coincides with the measured zero field data above $\simeq$25 K. This appears reasonable, because the zero-field c_{mag}^{0T} is expected to rapidly fall off above T_{C}. In principle, one could estimate c_{ph} by subtracting a zero field calculation of c_{mag}^{0T} from the respective measured data. The mean-field approximation neglects, however, the fluctuations around T_{C} and the gapless spinwave excitations at low temperatures, which strongly influence the temperature dependence of c_{mag} in zero field. Thus, we performed the mean-field calculation for a magnetic field of 14 T, which is large enough to broaden the transition strongly and to induce a sizable gap in the excitation spectrum.

Within a mean-field approximation the internal energy per mol formula units of a Heisenberg ferromagnet can be expressed by [9]

$$E = -\frac{3N_{\mathrm{A}}k_{\mathrm{B}}T_{\mathrm{C}}S}{2(S+1)}\frac{M^2}{M_{\mathrm{sat}}^2} - \mu_{\mathrm{B}}N_{\mathrm{A}}BM. \tag{1}$$

Here, N_{A} and k_{B} denote Avogadro's constant and Boltzmann's constant, respectively, $S = 1/2, 1, 3/2, \ldots$ is the spin number, μ_B the Bohr magneton, T_{C} the zero-field transition temperature and $M_{\mathrm{sat}} = 2\mu_B S$ the saturation magnetization. Thus, the only parameter to be calculated is the temperature- and magnetic-field-dependent magnetization $M(T, B)$. As described in standard textbooks [10], $M(T, B)$ follows from an implicit equation that can be solved numerically. From (1), the magnetic contribution to the molar heat capacity is calculated via

$$c_{\mathrm{mag}} = \frac{\partial E}{\partial T} = -\frac{3N_{\mathrm{A}}k_{\mathrm{B}}T_{\mathrm{C}}SM}{(S+1)M_0^2}\frac{\partial M}{\partial T} - \mu_{\mathrm{B}}N_{\mathrm{A}}B\frac{\partial M}{\partial T}, \tag{2}$$

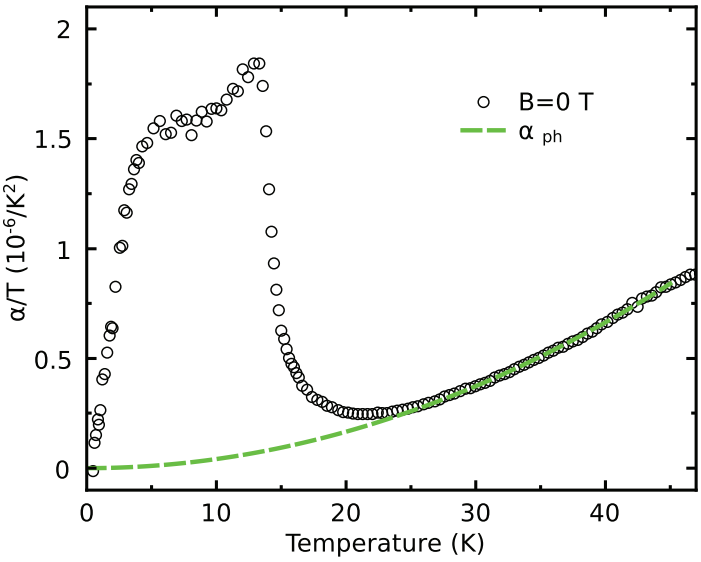

Figure 3. The zero-field thermal expansion of EuC_2 strongly resembles the corresponding specific heat data. The phonon contribution is estimated by a T^3 law $\alpha_{\rm ph} = AT^3$ with $A = 4.15 \times 10^{-10}\,{\rm K}^{-4}$.

and the magnetic entropy is obtained via integration $S_{\rm mag} = \int \frac{c_{\rm mag}(T)}{T} {\rm d}T$. The result can be used as a consistency check of the calculation, because $S_{\rm mag} = N_{\rm A} k_{\rm B} \ln(2S+1) \simeq 17.3\,{\rm J\,mol^{-1}\,K}$ has to be reached for all magnetic fields when the integration is done to large enough temperatures. The experimental magnetic entropy change of EuC_2 is obtained by the integration $\int \frac{c_{\rm tot}(T) - c_{\rm ph}(T)}{T} {\rm d}T$. For the zero-field data, this integration yields $S_{\rm mag} \simeq 17.6\,{\rm J\,mol^{-1}\,K}$, which is very close to the expected value of an $S = 7/2$ system.

Figure 3 displays the zero-field linear thermal expansion of EuC_2 in the representation α/T versus T. Obviously, the shape of this curve with a pronounced anomaly at $T_{\rm C} \simeq 14\,{\rm K}$ and a maximum around 4 K very strongly resembles the c_p^{0T}/T data shown in figure 2. For further analysis, we again assume the superposition of phononic and magnetic contributions $\alpha_{\rm tot} = \alpha_{\rm ph} + \alpha_{\rm mag}$ and estimate $\alpha_{\rm ph}$ by a quadratic fit of the zero-field $\alpha_{\rm ph}(T)/T$ data in the temperature range above 25 K (dashed line in figure 3). An approximate proportionality between thermal expansion and specific heat is often observed in solids and is related to the Grüneisen scaling, which can be straightforwardly derived from Maxwell's relations for systems that are determined by a single energy scale [11, 12]. The Heisenberg ferromagnet with nearest neighbour exchange J is such a system, and it has been shown explicitly [13–15] that the magnetic contributions of the specific heat and thermal expansion are expected to scale with each other with a proportionality constant that is determined by the pressure (or volume) dependence of J. Thus, the magnetic contribution of the thermal expansion coefficient can be expressed as

$$\alpha_{\rm mag} = \frac{\partial \ln J}{\partial p} \frac{c_{\rm mag}}{3V_{\rm mol}}. \tag{3}$$

The additional factor of 3 in the denominator takes into account that $\alpha_{\rm mag}$ is the linear thermal expansion, which in the case of a polycrystal is one-third of the volume expansion. Figure 4 compares the zero-field data of $\alpha_{\rm mag}$ and $c_{\rm mag}$, which are obtained by subtracting $\alpha_{\rm ph}$ and

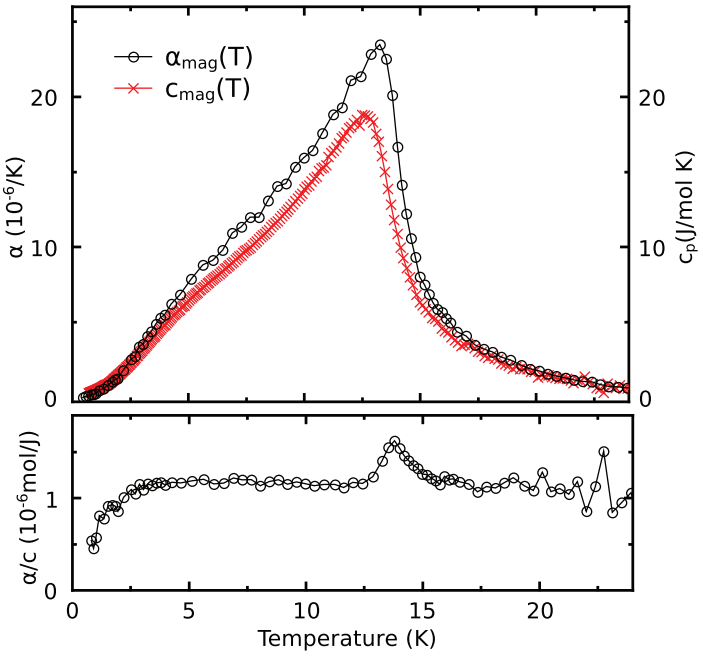

Figure 4. Magnetic contributions of the thermal expansion and specific heat (top) of EuC_2. The ratio α_{mag}/c_{mag} (bottom) is essentially constant in the entire temperature range, as expected from a Grüneisen scaling.

c_{ph} from the respective measurements. In the lower panel of this figure, we show the ratio $\alpha_{mag}(T)/c_{mag}(T)$, which is practically constant in the temperature range from about 2 to 22 K. The peak in the close vicinity of T_C may partly arise from small differences in the temperature calibrations of different experimental setups. An additional source of this deviation is differences in the critical behaviour of α_{mag} and c_{mag}.

The measurements of thermal expansion and specific heat also allow us to derive the initial slope of $\partial T_C/\partial p$ at ambient pressure. In the case of a second-order phase transition, this pressure dependence is given by the Ehrenfest relation

$$\left.\frac{\partial T_C}{\partial p}\right|_{p_0} = 3T_C V_{mol}\frac{\Delta\alpha}{\Delta c_p}, \tag{4}$$

where $\Delta\alpha$ and Δc_p denote the mean-field jumps of α and c_p, respectively. Because there are no sharp jumps in $\alpha(T)$ and $c_p(T)$, one could approximate the experimentally obtained anomalies by jumps using, e.g., area-conserving constructions, or it is possible to obtain a measure of $\partial \ln T_C/\partial p$ from a scaling of the anomalies of $\alpha(T)$ and $c_p(T)$ in the vicinity of T_C. This second possibility expresses a reformulation of (4) in the form of (3), where J is exchanged by T_C. Within mean-field theory T_C and J are proportional to each other and therefore $\partial \ln T_C/\partial p = \partial \ln J/\partial p$, meaning that (4) and (3) are equivalent. Although this strict equality will not be valid in reality due to the presence of fluctuations, one may expect an approximate equality of (4) and (3). As shown in the lower panel of figure 4 the ratio $\alpha_{mag}(T)/c_{mag}(T) \simeq 1.25 \times 10^{-6}\,\mathrm{mol\,J^{-1}}$ over most of the temperature range and increases to $\simeq 1.5 \times 10^{-6}\,\mathrm{mol\,J^{-1}}$ around T_C. Thus, using $V_{mol} \simeq 34\,\mathrm{cm^3\,mol^{-1}}$ we estimate the hydrostatic

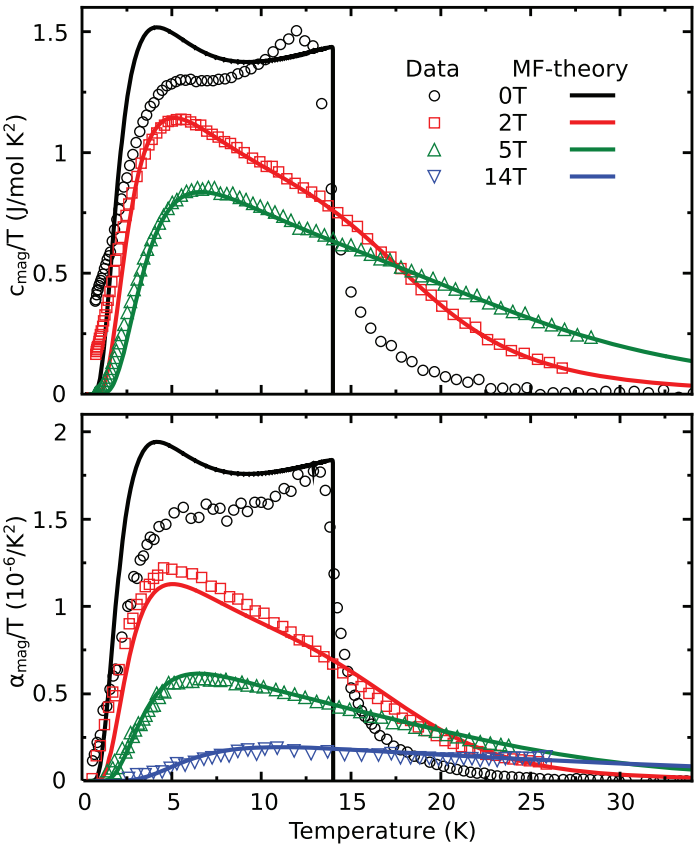

Figure 5. Magnetic contribution of the specific heat (top) and thermal expansion (bottom) of EuC_2 for different magnetic fields. The solid lines represent c_{mag} and α_{mag} calculated via (2) and (6), respectively.

pressure dependences

$$\left.\frac{\partial \ln T_C}{\partial p}\right|_{p_0} \simeq \left.\frac{\partial \ln J}{\partial p}\right|_{p_0} \simeq 0.14\,\mathrm{GPa}^{-1} \tag{5}$$

corresponding to an initial slope $\partial T_C/\partial p \simeq 2\,\mathrm{K\,GPa}^{-1}$. Thus, we conclude that external pressure should cause a strong increase of the ferromagnetic transition temperature of EuC_2 arising from a strong spin lattice coupling.

In the upper panel of figure 5, the experimental magnetic contribution of the specific heat measured for different magnetic fields is compared to the respective c_{mag} calculated via (2). As already mentioned, the mean-field calculation only yields a poor description of the zero-field data, because it reproduces neither the spin-wave contribution in the low-temperature region nor the behaviour around T_C. The experimental data obtained in 2 and 5 T are, however, rather well described, in particular in the high-temperature range. There are still deviations at low temperatures, but with increasing field these deviations decrease. Note that the data for 14 T are not shown here, because this measurement was used to estimate the phonon contribution c_{mag}.

The lower panel of figure 5 displays the magnetic contribution of the thermal expansion α_{mag} for different magnetic fields, which behaves very similarly to c_{mag}. For a ferromagnet with pressure-dependent exchange interaction, the mean-field theory predicts an anomalous length

change $\Delta L/L_0$, which is proportional to the squared magnetization $M^2(T)$ [14, 16]. Thus, for the magnetic thermal expansion $\alpha_{\rm mag} \propto M\frac{\partial M}{\partial T}$ is expected and, in order to emphasize the close analogy between $\alpha_{\rm mag}$ and $c_{\rm mag}$, we express the magnetic thermal expansion as

$$\alpha_{\rm mag} = -A \cdot \frac{3N_{\rm A}k_{\rm B}T_{\rm C}SM}{(S+1)}\frac{\partial M}{\partial T}. \tag{6}$$

This expression is identical to the first term of (2) multiplied by a constant factor A, which is determined by the scaling behaviour of the zero-field data shown in figure 4, i.e. $A = \alpha_{\rm mag}^{0T}/c_{\rm mag}^{0T} \simeq 1.25 \times 10^{-6}\,{\rm mol\,J^{-1}}$. Thus, all parameters of (6) are fixed and $\alpha_{\rm mag}$ calculated for different fields is shown by the solid lines in figure 5. Again, there are strong deviations concerning the zero-field data, whereas the agreement is already satisfactory for a field of 2 T and improves with increasing field. It is interesting to note that according to the mean-field equations (2) and (6) the scaling of the zero field $\alpha_{\rm mag}$ and $c_{\rm mag}$ is no longer valid in finite magnetic fields. This mean-field result is confirmed by the experimental data, despite the fact that the mean-field calculations do not reproduce the respective zero-field data: figure 4 confirms the scaling of the experimental zero-field data of $\alpha_{\rm mag}^{0T}$ and $c_{\rm mag}^{0T}$ and in figure 5 it is seen that this scaling changes in a finite magnetic field, because the flattening of the zero-field anomaly is more pronounced for $\alpha_{\rm mag}$ than for $c_{\rm mag}$.

From the thermodynamic data presented above, we find that the magnetization as well as the magnetic contributions of the specific heat and the thermal expansion are satisfactorily described within a mean-field theory assuming Eu^{2+} ions with localized $S = 7/2$ moments coupled via a pressure-dependent exchange coupling J. In particular, these data do not show any indications of field- or temperature-induced changes of the Eu valence, in agreement with the results of [7]. Mößbauer measurements carried out in the mentioned previous work detected a small but temperature-independent fraction of about 4–5% of Eu^{3+}. The $\simeq$4% reduction of the measured $\mu_{\rm sat}$ and $\mu_{\rm eff}$ compared to the expected values for an $S = 7/2$ system could also be explained by such an amount of Eu^{3+}, because Eu^{3+} only has a weak paramagnetic van Vleck susceptibility. It is, however, unclear whether such an Eu^{3+} content is an intrinsic property of EuC_2, since it might also arise from a sample-dependent off-stoichiometry and/or a weak oxygen contamination. The influence of weak off-stoichiometries is also the subject of intensive study in the closely related EuO, see e.g. [17], and it is found that the electrical resistivity can be drastically changed by weak variations of the Eu/O ratio. If EuC_2 is considered as a purely ionic compound composed of Eu^{2+} and C_2^{2-} ions, a semiconducting behaviour would be expected over the entire temperature. This simple ionic picture is, however, contradicted by the measured resistivity $\rho(T)$, showing an insulator-to-metal transition that coincides with the ferromagnetic ordering in zero field [7]. Moreover, EuC_2 shows a giant magnetoresistance effect in finite magnetic fields with resistivity changes of several orders of magnitude around $T_{\rm C}$. Thus, EuC_2 behaves very similarly to EuO.

In order to get more insight into the influence of stoichiometry, the synthesis of $EuC_{2\pm\delta}$ samples was performed. Figure 6 compares the resistivity of two nominally stoichiometric EuC_2 samples and two off-stoichiometric samples that are expected to be either Eu or C_2 deficient, i.e. nominally electron- or hole-doped. The qualitative behaviour for all samples is rather similar. Upon decreasing the temperature down to $T_{\rm C}$, the resistivity continuously increases and then $\rho(T)$ strongly decreases below $T_{\rm C}$ and finally becomes practically temperature independent below about 7 K. Based on the opposite temperature dependences above and

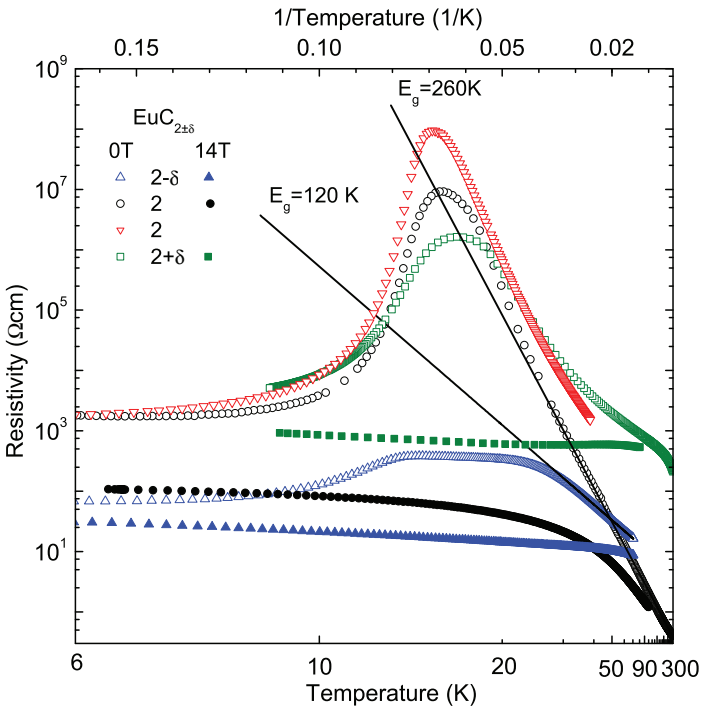

Figure 6. Arrhenius plot of the resistivity of various $EuC_{2\pm\delta}$ samples prepared for different E/C ratios (see text). The open symbols represent the data in zero magnetic field and the corresponding filled symbols show measurements in a field of 14 T. The black lines specify the curves for constant activation energies E_g. It is notable that the off-stoichiometric samples have a considerably smaller E_g.

below T_C, one may discuss this as an insulator-to-metal transition, but in view of the rather large absolute values of ρ below T_C, it is also appropriate to consider an insulator-to-insulator transition. Concerning the maxima, the nominally stoichiometric samples reach $\rho \gtrsim 10^7\,\Omega\,\mathrm{cm}$. The maximum for the nominally Eu-deficient sample is still larger than $10^6\,\Omega\,\mathrm{cm}$, while in the C_2-deficient sample a broadened plateau is observed with $\rho(T) \simeq 10^2\,\Omega\,\mathrm{cm}$ in the temperature range from about 12 to 20 K. Moreover, the low-temperature resistivity of $EuC_{2-\delta}$ is about one order of magnitude lower than ρ of the other samples. In the temperature range above 30 K, the resistivity of all samples decreases more or less linearly in the Arrhenius plot, i.e. there is an activated behaviour $\rho(T) \propto \exp(E_g/k_B T)$ with a temperature-independent activation energy E_g. It is remarkable that both off-stoichiometric samples have a similar $E_g \approx 120\,\mathrm{K}$ in the paramagnetic phase, whereas the stoichiometric samples have a significantly larger activation energy $E_g \approx 260\,\mathrm{K}$. This suggests that variations in the stoichiometry induce donator or acceptor levels in the bandgap, which may strongly influence the resistivity behaviour, but the influence on the ferromagnetic ordering temperature is comparatively weak. At the present stage of sample preparation and characterization, it is not possible to give a precise determination of the real composition of the studied samples, which would be necessary to estimate the charge-carrier content. The magnetization curves of the off-stoichiometric samples suggest that the charge carrier content varies by only a few per cent, because μ_{sat} and μ_{eff} vary by $\approx 4\%$.

This, together with the fact that no single-crystalline samples are available, prevents a deeper analysis of the complex resistivity behaviour of the different samples shown in figure 6.

Concerning the resistivity data of the off-stoichiometric samples in 14 T, we find that the GMR effect is smaller than for the stoichiometric ones. Whereas the resistivity of EuC_2 decreases about five orders of magnitude at the ferromagnetic transition, it decreases only three orders for $EuC_{2+\delta}$ and one order for $EuC_{2-\delta}$. It is obvious that the magnetoresistance strongly depends on the maximum value of resistivity in zero field.

In many aspects the data of $EuC_{2\pm\delta}$ resemble the early investigations of the Eu chalcogenides EuS and EuO [18–21]. There, it was also observed that, depending on the exact preparation process and/or subsequent tempering procedures, the resistivity may vary over several orders of magnitude, in particular in the temperature range of the ferromagnetic ordering temperature. This has been attributed to the influence of donator and/or acceptor levels, which are controlled by the exact stoichiometry. The occurrence of an insulator-to-metal transition at the ferromagnetic ordering of EuO is explained by an exchange splitting of the conduction band into spin-up and spin-down bands, which is large enough to drop one of these bands below the donator levels [17]. This means, however, that a finite quantity of donator levels is required to make the ferromagnetic state conducting. The different orders of magnitude of the jumps in resistivity and the huge CMR could be quantitatively reproduced within an extended Kondo lattice model [22]. The decisive parameter in this model, for the big variations in the resistivity behaviour, is the oxygen vacancy concentration. In most aspects, our data of EuC_2 strongly resemble the corresponding data of EuO.

4. Summary

We have investigated the magnetization, specific heat, thermal expansion and resistivity of high-quality EuC_2 samples. The temperature and field dependences of the magnetization fit the magnetic moment expected for Eu^{2+} ions with $S = 7/2$. The specific heat $c_p(T)$ and the thermal expansion $\alpha(T)$ show well-defined anomalies at the magnetic phase transition and the magnetic contributions of c_{mag} and α_{mag} could be extracted for further analysis. Using Ehrenfest's relation to determine the pressure dependence of the Curie temperature, an initial slope of $\partial T_{\mathrm{C}}/\partial p \simeq 2\,\mathrm{K\,GPa^{-1}}$ is found. The zero-field data of c_{mag} yield a magnetic entropy $S_{\mathrm{mag}} \simeq 17.6\,\mathrm{J\,mol^{-1}\,K}$, which is close to the expected value of an $S = 7/2$ system. The ratio $\alpha_{\mathrm{mag}}/c_{\mathrm{mag}}$ is practically constant in the temperature from about 2 to 22 K, meaning that the respective zero-field data obey a magnetic Grüneisen scaling. This Grüneisen scaling is, however, not preserved in finite magnetic fields. Comparing the experimentally obtained magnetic contributions c_{mag} and α_{mag} to the respective results calculated within a mean-field model for an $S = 7/2$ system, we find that the experimental data for larger magnetic fields are well reproduced by the mean-field model, whereas the calculations for zero field only yield a poor description of the experimental data. Nevertheless, the mean-field model correctly predicts that the zero-field Grüneisen scaling is no longer valid in finite fields. The influence of weak off-stoichiometries was studied by comparing the resistivity measurements of nominally stoichiometric EuC_2 and off-stoichiometric samples, which are expected to be either Eu or C_2 deficient. The variations in the stoichiometry most probably induce donator or acceptor levels in the bandgap, which strongly affects the resistivity behaviour, whereas the influence on T_{C} is comparatively weak. In all these aspects the resistivity data strongly resemble the early investigations of the Eu chalcogenide EuO.

Acknowledgments

This work was supported by the Deutsche Forschungsgemeinschaft through Schwerpunktprogramm 1166 and Sonderforschungsbereich 608.

References

[1] Gulden Th, Henn R W, Jepsen O, Kremer R K, Schnelle W, Simon A and Felser C 1997 *Phys. Rev.* B **56** 9021
[2] Long J R, Hoffmann R and Meyer H-J 1992 *Inorg. Chem.* **31** 1734
[3] Long J R, Halet J-Y, Saillard J-Y, Hoffmann R and Meyer H-J 1992 *New J. Chem.* **16** 839
[4] Gebelt R E and Eick H A 1964 *Inorg. Chem.* **3** 335
[5] Sakai T, Adachi G, Yoshida T, Ueno S and Shiokawa J 1982 *Bull. Chem. Soc. Japan* **55** 699
[6] Faircloth R L, Flowers R H and Pummery F C W 1968 *J. Inorg. Nucl. Chem.* **30** 499
[7] Wandner D, Link P, Heyer O, Mydosh J, Ahmida M A, Abd-Elmeguid M M, Speldrich M, Lueken H and Ruschewitz U 2010 *Inorg. Chem.* **49** 312
Wandner D *et al* 2011 *Inorg. Chem.* **50** 2703
[8] Rotter M, Loewenhaupt M, Doerr M, Lindbaum A and Michor H 2001 *Phys. Rev.* B **64** 14402
[9] Fernandez Rodriguez J and Blanco J A 2005 *Phys. Scr.* **71** CC19
[10] Blundell S 2001 *Magnetism in Condensed Matter (Oxford Master Series)* (Oxford: Oxford University Press)
[11] Zhu L, Garst M, Rosch A and Si Q 2003 *Phys. Rev. Lett.* **91** 066404
[12] Lorenz T, Stark S, Heyer O, Hollmann N, Vasiliev A, Oosawa A and Tanaka H 2007 *J. Magn. Magn. Mater.* **316** 291
[13] Mattis D C and Schultz T D 1963 *Phys. Rev.* **129** 175
[14] Callen E and Callen H B 1965 *Phys. Rev.* **139** A455
[15] Argyle B E, Miyata N and Schultz T D 1967 *Phys. Rev.* **160** 413
[16] Chikazumi S 1997 *Physics of Ferromagnetism Int. Series of Monographs on Physics* (Oxford: Oxford University Press)
[17] Steeneken P G, Tjeng L H, Elfimov I, Sawatzky G A, Ghiringhelli G, Brookes N B and Huang D-J 2002 *Phys. Rev. Lett.* **88** 047201
[18] Shapira Y and Reed T B 1972 *Phys. Rev.* B **5** 4877
[19] Shapira Y, Foner S and Reed T B 1973 *Phys. Rev.* B **8** 2299
[20] Oliver M R, Dimmock J O, McWhorter A L and Reed T B 1972 *Phys. Rev.* B **5** 1078
[21] Mauger A and Godart C 1980 *Solid State Commun.* **35** 785
[22] Sinjukow P and Nolting W 2003 *Phys. Rev.* B **68** 125107